2014

Effective Flow And Force Areas Of Discharge Valve In A Rotary Compressor

Qin Tan
Xi'an Jiaotong University, China, People's Republic of, tanqin@stu.xjtu.edu.cn

Zhan Liu
Xi'an Jiaotong University, China, People's Republic of, lzlp68@163.com

Junming Cheng
Xi'an Jiaotong University, China, People's Republic of, cjm1878@163.com

Quanke Feng
Xi'an Jiaotong University, China, People's Republic of, qkfeng@mail.xjtu.edu.cn

Effective Flow and Force Areas of Discharge Valve in a Rotary Compressor

Qin TAN, Zhan LIU, Junming CHENG, Quanke FENG*

School of Energy and Power, Xi'an Jiaotong University, Xi'an, China
E-mail: qkfeng@mail.xjtu.edu.cn

* Corresponding Author

ABSTRACT

In this paper, two fluid–structure interaction (FSI) models of the discharge valve are presented to study the effect of partly covering the discharge port by the cylinder and the roller on the effective flow and force areas. One is the full FSI model and another is the simplified FSI model in which the discharge port is not covered and the cylinder shape is simplified to be cylindrical. The pressure in the compression chamber, the displacement of the valve reed, the volumetric flow rate through the valve and the gas force acting on the valve reed head are obtained by the two FSI model. The results comparison between the two FSI models shows the effective flow and force area in the full FSI model are much different from those in the simplified FSI model. The factors which affect the covering area of the discharge port must be taken into consideration in the calculations of these two areas.

1. INTRODUCTION

Discharge valve of rotary compressor is a reed type valve, which consists of a valve seat, a valve reed and a retainer. Usually, the discharge process was assumed as a one-dimensional flow through an orifice in the mathematical model of the valve (Prater and Ratterman, 1992; Huang and Xie, 2008).The effective flow area was proposed to build relationship between the pressure drop across the valve and the mass flow rate in the flow equation, and the effective force area was used to build relationship between the pressure drop across the valve and the gas force acting on the valve reed surface in the dynamic equation. The precision of the valve model depends largely on the accuracy of these two areas.

A number of investigators have conducted experiments to study the effective flow and force areas of the reed valve (Wambsganss and Cohen, 1967; Soedel, 1972; Deschamps et al., 1988). In their experiments, the fluid was discharged directly through the discharge port, and the flow into the discharge port was uniform. The results are reliable for a reciprocating compressor valve rather than for a rotary compressor valve, because the discharge port is covered partly by the cylinder and the roller in the rotary compressor, and the flow is non-uniform during the discharge process.

Much numerical works have been conducted to study the transient gas flow in the rotary compressor by CFD approach and moving mesh technology (Liu and Geng, 2004; Geng et al., 2004; Liang et al., 2010), It is convenient to gain effective flow and force areas more accurately by such simulations. In addition, with the rapid development of fluid–structure interaction (FSI) method, three-dimensional FSI model of the reed valve has been wildly used in the reciprocating compressor (Kim et al., 2006; Kim et al., 2008; Choi et al., 2010; Mistry et al., 2012).

In this paper, two three-dimensional FSI models for the discharge valve in the rotary compressor are presented. One is the full FSI model and another is the simplified FSI model in which the discharge port is not covered and the cylinder shape is simplified to be cylindrical. By comparing results between these two FSI models, the effect of partly covering the discharge port by the cylinder and the roller on the effective flow and force areas is studied. The conclusion is important to develop a precise mathematical model of the discharge valve in a rotary compressor.

2. FSI MODEL

2.1 Discharge process in a rotary compressor

The working chamber of a rotary compressor shown in Figure 1 is divided into a suction chamber and a compression chamber by a vane. When the pressure in the compression chamber is higher than the pressure outside the cylinder, the valve is opened and then the refrigerant is discharged through the oblique incision and the discharge port. Figure 1 also shows the profile of the discharge port when the rotor rotational angle θ is θ1 degree and 360-θ2 degree. It can be seen that the discharge port begins to be covered partly by the roller as the rotor rotational angle rises up to a certain angle. And it is always covered partly by the cylinder. In this study, the rotational speed of the compressor is 4800 r/min.

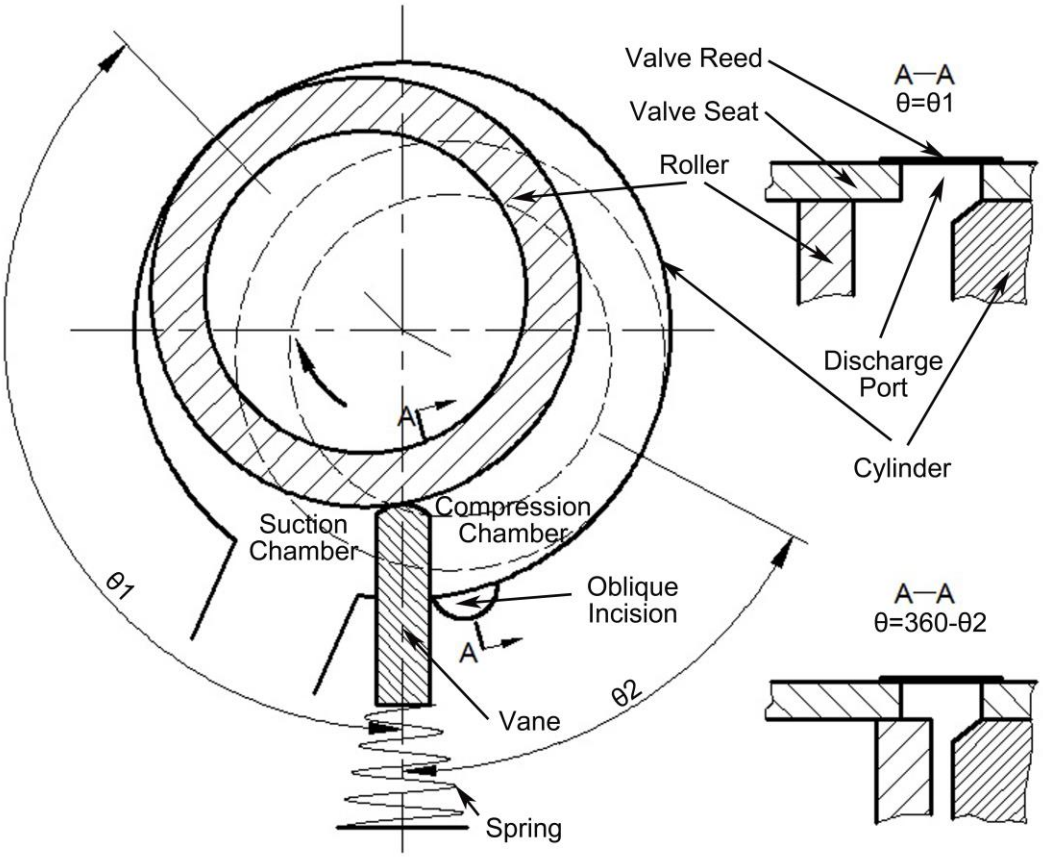

Figure 1: Schematic diagram of the rotary compressor

2.2 Governing equations

2.2.1. Governing equations of the fluid domain: The governing equations for fluid flow consist primarily of the Navier–Stokes equations. In a fixed Cartesian coordinate frame of reference, they are expressed in conservative forms for mass, momentums and energy respectively

$$\frac{\partial \rho}{\partial t} + \nabla \cdot (\rho \mathbf{v}) = 0 \tag{1}$$

$$\frac{\partial \rho \mathbf{v}}{\partial t} + \nabla \cdot (\rho \mathbf{v}\mathbf{v} - \boldsymbol{\tau}) = \mathbf{f} \tag{2}$$

$$\frac{\partial \rho E}{\partial t} + \nabla \cdot (\rho \mathbf{v} E - \boldsymbol{\tau} \cdot \mathbf{v} + \mathbf{q}) = \mathbf{f} \cdot \mathbf{v} + q \tag{3}$$

where, ρ is the density, t is the time, $\mathbf{v}$ is the velocity vector, $\boldsymbol{\tau}$ is the stress tensor, $\mathbf{f}$ is the body force vector, E is the specific total energy, $\mathbf{q}$ is the heat flux vector and q is the rate of heat generation.

2.2.2. Governing equations of the solid domain: The equation of structural dynamics is used to describe the discharge valve motion. The governing equilibrium equation at time $t+\Delta t$ is given by, in implicit time integration,

$$\mathbf{M}\ddot{\mathbf{U}}^{t+\Delta t} + \mathbf{C}\dot{\mathbf{U}}^{t+\Delta t} + \mathbf{K}^{t}\mathbf{U} = \mathbf{R}^{t+\Delta t} - \mathbf{F}^{t} \tag{4}$$

where $\mathbf{M}$ is the mass matrix, $\ddot{\mathbf{U}}^{t+\Lambda t}$ and $\dot{\mathbf{U}}^{t+\Lambda t}$ are respectively the nodal point acceleration vector and the nodal point velocity vector at time $t+\Delta t$, $\mathbf{U}$ is the nodal point displacement vector increments from time t to time $t+\Delta t$, $\mathbf{C}$ is the damping matrix, $\mathbf{K}^{t}$ is the stiffness matrix at time t, $\mathbf{R}^{t+\Lambda t}$ is the external load vector at time $t+\Delta t$, $\mathbf{F}^{t}$ is the nodal point force vector at time t.

Contact conditions must be specified to simulate the contact processes occurring at the surfaces of the valve. The normal contact conditions can be expressed as (Eterovic and Bathe, 1991)

$$g \geq 0\,,\ \lambda \geq 0\,,\ g\lambda = 0 \tag{5}$$

where g is the distance between two contacting bodies and λ is the normal contact pressure.

2.2.3. Equations of fluid–structural interaction: The fundamental conditions applied to the fluid-structure interfaces are the kinematic condition and the dynamic condition, which can be written as follows

$$\underline{\mathbf{d}}_f = \underline{\mathbf{d}}_s \tag{6}$$

$$\mathbf{n} \cdot \underline{\boldsymbol{\tau}}_f = \mathbf{n} \cdot \underline{\boldsymbol{\tau}}_s \tag{7}$$

where $\underline{\mathbf{d}}_f$ and $\underline{\mathbf{d}}_s$ are, respectively, the fluid and solid displacement, $\underline{\boldsymbol{\tau}}_f$ and $\underline{\boldsymbol{\tau}}_s$ are, respectively, the fluid and solid stress. $\mathbf{n}$ is the unit boundary normal vector outwards from computational domain. Variables in the fluid and solid domain are fully coupled. The fluid and solid equations are solved individually using the latest data provided from each other.

2.3 Finite element model

Table 1: Dimensions of the compressor.

Component	Length (mm)
Cylinder height	20
Cylinder diameter	38.9
Roller outer diameter	30.56
Vane width	3.2
Discharge port diameter	6.5

The rotary compressor studied in this paper has a working chamber volume of 9.1 cm^3. Dimensions of the rotary compressor and the discharge valve are shown in Table 1 and Fig. 2, respectively. In the full FSI model, the computation domain is divided into the fluid domain and the solid domain. The suction port, the cylinder volume and the discharge chamber are considered as the fluid domain, while the discharge valve is taken as the solid domain. 3D 8-node brick elements are used to mesh the fluid and solid domains while 3D 4-node tetrahedron elements are for the suction port. The initial finite element model of the fluid domain and the discharge valve are shown in Fig. 3.

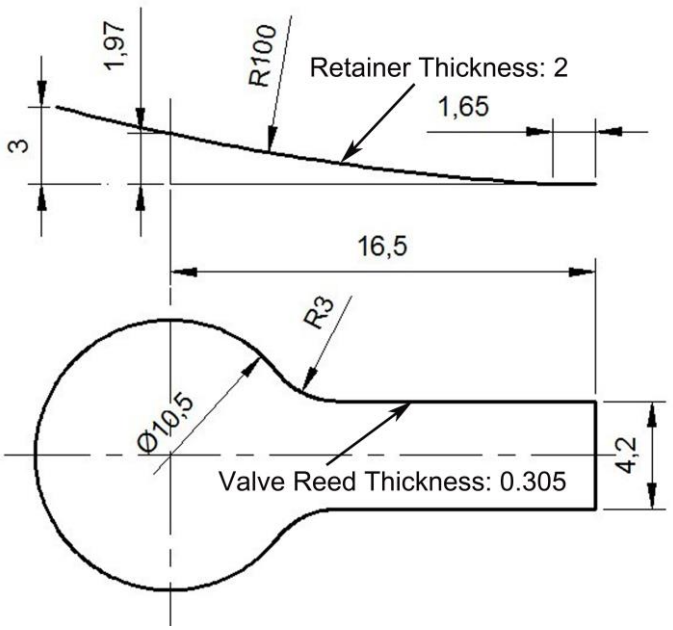

Figure 2: Dimensions of the discharge valve

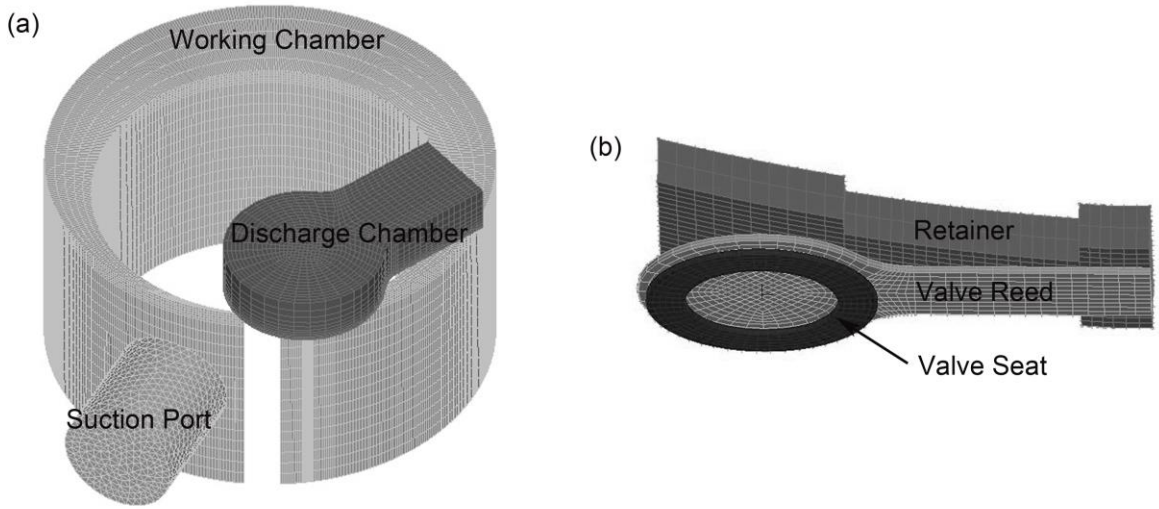

Figure 3: Initial finite element models of the full FSI model: (a) the fluid domain, (b) the discharge valve.

To demonstrate effects of partly covering the discharge port by the cylinder and the roller on the effective flow and force areas, another FSI model named simplified FSI model is specially presented. Its cylinder is cylindrical, as shown in Fig.4. The fluid in the compression chamber of this model can be discharged directly through the discharge port without being covered. The volumetric change rate of cylinder is set to be the same in the two FSI models.

The working fluid is R410A and the valve reed is made of Sandvik 7C steel. In the fluid domain, the pressure and temperature at the inlet of the suction port are given as 0.9978 MPa and 308.15 K, respectively. The pressure at the outlet of the discharge chamber is given as 3.385 MPa. The two FSI model is created using the commercial multiphysics code ADINA 8.8(ADINA, 2011).

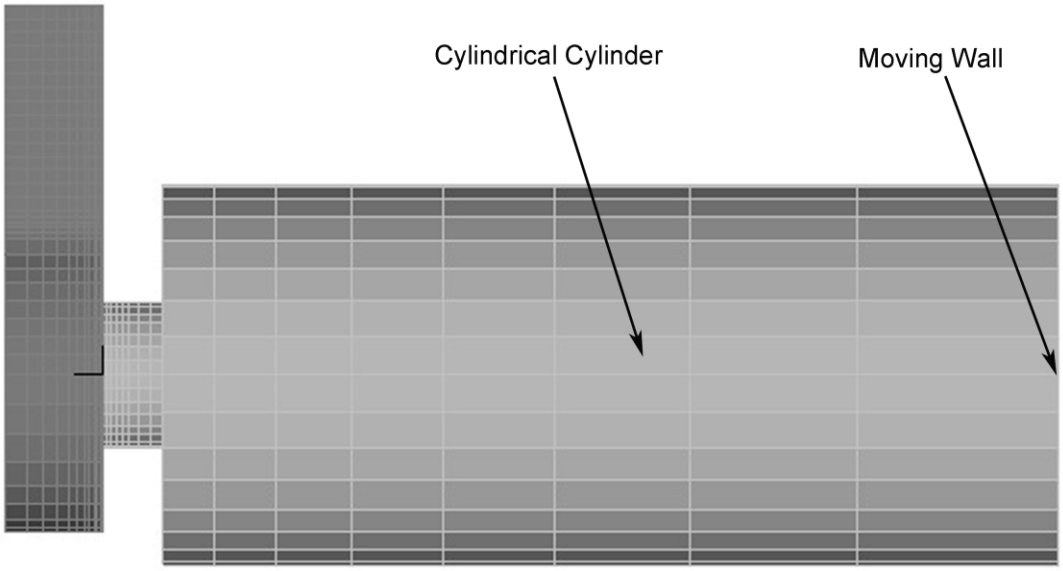

Figure 4: Fluid model of the simplified FSI model

3. RESULTS AND DISCUSSION

Compression chamber pressure of the full FSI model and the simplified FSI model are shown in Fig. 5. The pressure tracking points are set at the lower surfaces of compression chambers. The flow energy loss through the discharge valve by the full FSI model is 46.54 W, while that by the simplified FSI model is only 37.31 W. The explanation of quite such a difference is that the fluid in the compression chamber of the simplified FSI model is easier to be discharged than that of the full FSI model because its discharge port is not covered by the cylinder and the roller.

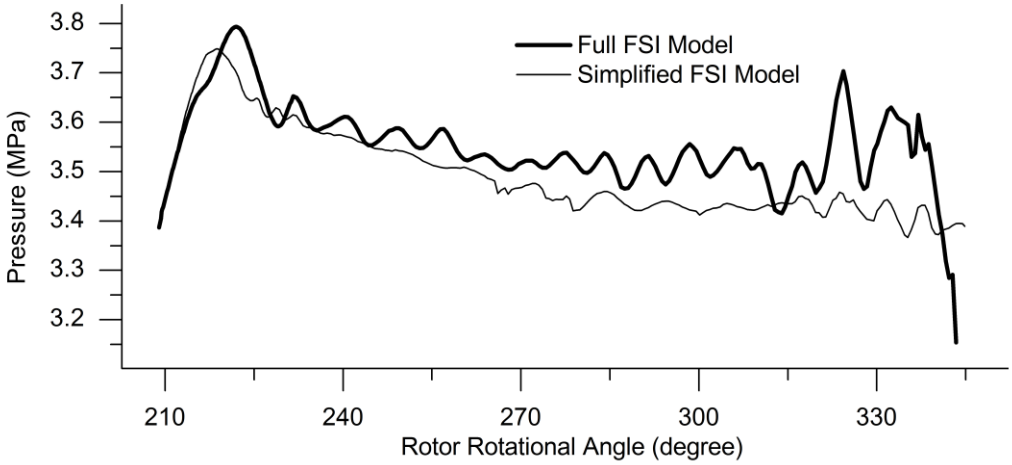

Figure 5: P-θ diagrams of the full FSI model and the simplified FSI model

Comparisons of the displacement and the velocity of the point h0 located at the center of valve reed head, the gas force acting on the valve reed head and the volumetric flow rate through the valve between the two FSI models are displayed in Fig. 6. It can be seen that the velocity of the valve reed impacting on the retainer in the full FSI model is 3.7 m s^{-1} smaller than that in the simplified FSI model. And the gas force and the volumetric flow rate in the simplified FSI model is larger than that in the full FSI model at the initial valve-opening period, but become close at later period of the discharge process.

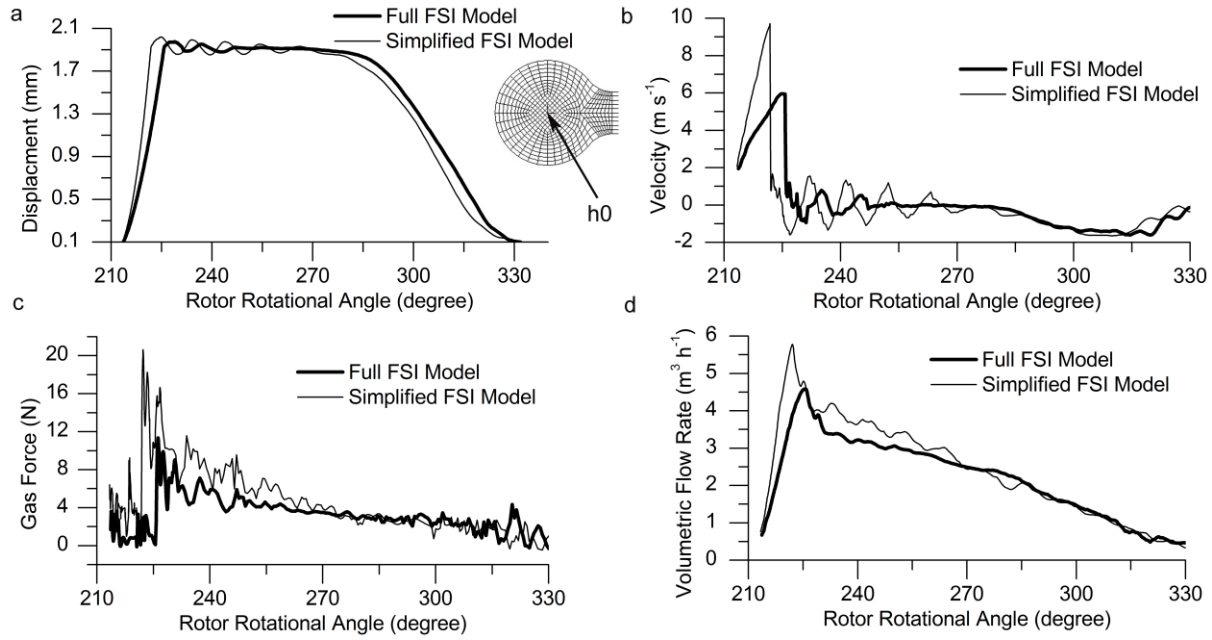

Figure 6: Comparison between the full FSI model and the simplified model: (a) displacement, (b) velocity, (c) gas force, (d) volumetric flow rate

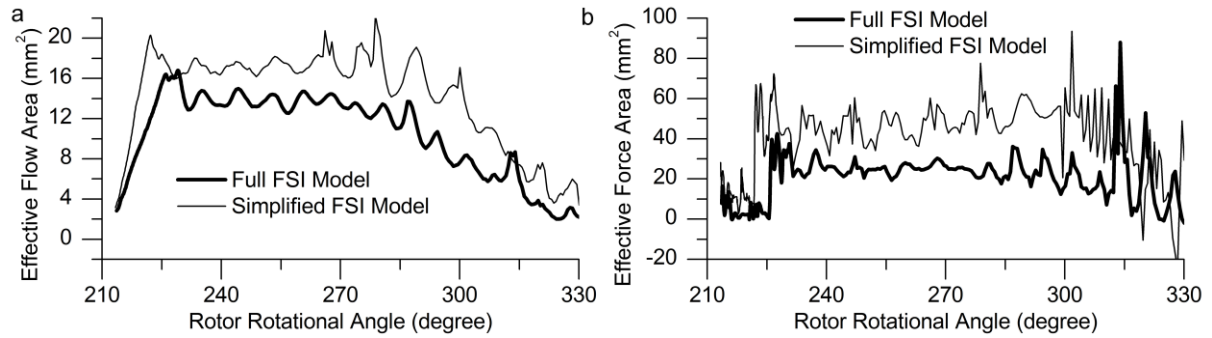

Figure 7: Comparison between the full FSI model and the simplified model: (a) effective flow area, (b) effective force area

The effective flow and force area shown in Figure 7 can be calculated as follows, respectively

$$A_{ef} = \dot{m}_V / \sqrt{2(p_c - p_d)/\rho} \tag{12}$$

$$A_{ep} = F_{gas} / (p_c - p_d) \tag{13}$$

where A_{ef} and A_{ep} mean the effective flow area and effective force area respectively, $\dot{m}_V$ means volumetric flow rate, F_{gas} means gas force acting on the valve reed head, p_c means pressure in the compression chamber, and P_d means discharge pressure. The comparison is meaningful only under condition that the flow and force areas are the same in the two models. So the comparison given in Table 2 is made at the time when the displacement of the point h0 is approximate in the two models (h is the displacement of the point h0). It shows the effective flow and force areas in the simplified FSI model are much larger than that in the full FSI model. And the effective flow area declines obviously after the roller covers the discharge port in the full FSI model. For example, the effective flow area decreases to 3.67 from 7.27 and the ratio goes up to 2.14 from 1.13 when h is 0.5 mm. So because the discharge port is covered partly by the cylinder and the roller, the effective flow and force area are significantly affected. The rotor rotational angle, which determines the covered area of discharge port, must be taken into consideration in the calculation of the effective flow and force areas.

Table 2: Comparison of effective flow and force areas between the full FSI model and the simplified FSI model

h (mm)	Model	θ (degree)	A_{ef}	A_{ep}	$\frac{A_{ef,sfsi}}{A_{ef,ffsi}}$	$\frac{A_{ep,sfsi}}{A_{ep,fsi}}$
0.5	SFSI	216.5	8.23	11.5	1.13	10.0
	FFSI	217.6	7.27	1.15		
0.7	SFSI	217.4	10.41	11.17	1.19	4.62
	FFSI	220.0	8.74	2.42		
1.4	SFSI	220.2	16.47	10.58	1.24	1.48
	FFSI	223.2	13.23	7.16		
1.9	SFSI	241.3	17.27	44.26	1.16	2.02
	FFSI	244.9	14.84	21.95		
1.4	SFSI	296.1	14.24	51.23	1.94	4.15
	FFSI	299.0	7.34	12.34		
0.5	SFSI	313.3	7.86	36.84	2.14	6.81
	FFSI	317.4	3.67	5.41		

Figure 7 (b) and Table 2 show the effective force area at the initial valve-opening period is much smaller than that at later period of the discharge process(the valve reed rise and fall at these two periods, respectively). For instance, the effective force area increases to 36.84 from 7.16 for the full FSI model when h is 1.4 mm. And the effective force area increase suddenly while the valve reed impact the retainer. It reveals that the velocity of the valve reed have a great influence on the effective force area.

4. CONCLUSION

Partly covering the discharge port by the cylinder and roller can not be neglected in the research of the effective flow and force areas of the reed valve for the rotary compressor. Otherwise, the two areas will much larger than that in the real compressor. If such imprecise two areas are used in the valve model, the flow energy loss through the discharge valve will be underestimated, and the impact stress and the impact velocity of the valve reed impacting on the retainer will be an excessively high value. More experiments and simulations need to be conducted to determine the relationship between these two areas and the factors which determine the covering area of the discharge port, such as size of the oblique incision and the rotor rotational angle.

REFERENCES

ADINA R&D, Inc., 2011. ADINA System 8.8 Documentation.

Choi, Y.-S., Lee, J.-H., Jeong, W.-B., Kim, I.-G., 2010, Dynamic behavior of valve system in linear compressor based on fluid-structure interaction, *J. Mech. Sci. Technol*., vol. 24, no. 7: p. 1371-1377.

Deschamps, C.J., Ferreira, R.T.S., Prata, A.T., 1988, The Effective Flow and Force Areas in Compressor Valves, *In: 1988 International Compressor Engineering Conference at Purdue*, p. 104-111.

Eterovic, A.L., Bathe, K.J., 1991, On the Treatment of Inequality Constraints Arising from Contact Conditions in Finite Element Analysis, *Comput. Struct*., vol. 40, no. 2: p. 203-209.

Geng, W., Liu, C., Wang, Y., 2004, The Performance Optimization of Rolling Piston Compressors Based on CFD Simulation, *In: 17th International Compressor Engineering Conference at Purdue*, C013.

Huang, B., Xie, F., 2008, Dynamic Analysis of the Discharge Valve of the Rotary Compressor, *In: 19th International Compressor Engineering Conference at Purdue*, 1182.

Kim, H.-S., Ahn, J.-W., Kim, D.-H., 2008, Fluid Structure Interaction and Impact Analyses of Reciprocating Compressor Discharge Valves, *In: 19th International Compressor Engineering Conference at Purdue*, 1112.

Kim, J., Wang, S., Park, S., Ryu, K., La, J., 2006, Valve Dynamic Analysis of a Hermetic Reciprocating Compressor, *In: 18th International Compressor Engineering Conference at Purdue*, C107.

Liang, S., Kang, X., Liu, Q., Zhou, P., Xia, S., Hu, Y., 2010, Investigation of Refrigerant Flow Simulation and Experiment of Rolling Piston Compressors, *In: 20th International Compressor Engineering Conference at Purdue*, 1164.

Liu, C., Geng, W., 2004, Research on Suction Performance of Two-cylinder Rolling Piston Type Rotary Compressors Based on CFD Simulation, *In: 17th International Compressor Engineering Conference at Purdue*, C101.

Mistry, H., Bhakta, A., Dhar, S., Bahadur, V., Dey, S., 2012, Capturing Valve Dynamics in Reciprocating Compressors through Computational Fluid Dynamics, *In: 21st International Compressor Engineering Conference at Purdue*, 1210.

Prater, G.Jr., Ratterman, E.E., 1992, Development of a Computer Simulation Program for the Acoustic Tuning of Rolling Piston Compressors, *In: 1992 International Compressor Engineering Conference at Purdue*, C-6.

Soedel, W., 1972, Introduction to computer simulation of positive displacement type compressor, Purdue University.

Wambsganss, M.W.Jr., Cohen, 1967, Dynamic of reciprocating compressors with automatic reed valves, *In: Proceedings of XIIth International Congress of Refrigeration*, paper no. 3.06.

ACKNOWLEDGMENTS

This work is supported by the National Natural Science Foundation of China [NO.51106121].